Polymer Chemistry

Accelerated Hydrolytic Degradation of Ester-containing Biobased Epoxy Resins

Journal:	*Polymer Chemistry*
Manuscript ID	PY-ART-02-2019-000240.R1
Article Type:	Paper
Date Submitted by the Author:	26-Apr-2019
Complete List of Authors:	Shen, Minjie; University of Houston, Chemical and Biomolecular Engineering Almallahi, Rawan; University of Houston, Chemical and Biomolecular Engineering Rizvi, Zeshan; University of Houston, Chemical and Biomolecular Engineering Gonzalez, Eliud; University of Houston, Chemical and Biomolecular Engineering Yang, Guozhen; University of Massachusetts Amherst, Chemical Engineering Robertson, Megan; University of Houston, Chemical and Biomolecular Engineering

SCHOLARONE™
Manuscripts

Accelerated Hydrolytic Degradation of Ester-containing Biobased Epoxy Resins

*Minjie Shen,[a] Rawan Almallahi,[a] Zeshan Rizvi,[a,b] Eliud Gonzalez-Martinez,[a,b] Guozhen Yang,[a] and Megan L. Robertson[ac]**

[a] Department of Chemical and Biomolecular Engineering, University of Houston, 4726 Calhoun Road, Houston, TX 77204-4004, United States
[b] Houston Community College, Houston, TX 77082, United States
[c] Department of Chemistry, University of Houston, Houston, TX 77204-4004, United States

*Corresponding author
Megan Robertson
4726 Calhoun Road
S222 Engineering Building 1
University of Houston
Houston, TX 77204-4004
mlrobertson@uh.edu
713-743-2748

KEYWORDS: thermoset polymers, ester hydrolysis, polyesters, sustainable and biobased polymers, lignin, vegetable and triglyceride oils

Abstract

The accelerated hydrolytic degradation of biobased epoxy resins containing ester linkages was investigated. Epoxidized biobased molecules were utilized as sustainable replacements for the diglycidyl ether of bisphenol A (DGEBA) as an epoxy monomer, including epoxidized vanillic acid (EVA, derived from lignin), epoxidized plant-based phenolic acids (epoxidized salicylic acid, ESA, and 4-hydroxybenzoic acid, E4HBA), and epoxidized soybean oil (ESO). All biobased epoxy monomers contain esters (3 per molecule for ESO and 1 per molecule for EVA, ESA and E4HBA), in contrast to DGEBA (containing no esters). The epoxidized molecules were cured through reaction with an anhydride curing agent. Epoxy resins derived from EVA, ESA, and E4HBA exhibited comparable glass transition temperatures to that of the DGEBA-based epoxy resin. All biobased epoxy resins underwent rapid degradation in a basic solution as compared to the conventional DGEBA-based epoxy resin. ESO- and ESA-based epoxy resins exhibited the fastest degradation rates, whereas E4HBA- and EVA-based epoxy resins exhibited more moderate degradation rates. Variations in degradation rate are attributed to differences in epoxide content, monomer structure, degree of hydrophilicity, crosslink density, and proximity to glass transition temperature. The degradation profiles, mass loss as a function of exposure time in the basic solution, showed good agreement with predictions from a solid-state kinetic model. Mass spectrometry and scanning electron microscopy analyses confirmed the epoxy resins underwent hydrolytic degradation, through a surface erosion mechanism.

1. Introduction

The production of polymers has rapidly increased in past decades, and the majority of generated polymers ultimately reside in landfills at the end of their useful lifetime.[1] There is therefore a great need to recycle or reuse polymers in order to minimize their negative environmental impact. Thermoset polymers present unique challenges for recycling, as they are crosslinked and cannot be recycled with traditional methods for thermoplastics that employ melt processing. While an alternative approach is to depolymerize the materials back to their original constituents (i.e. chemical recycling),[2] most conventional thermoset polymers do not have the needed functionality to undergo these processes under benign conditions.[3] Epoxy resins are an important class of thermoset polymer, with wide ranging applications in coatings, adhesives, aircraft parts, automobile parts, insulation, building materials and wind turbine blades, among others.[4] Furthermore, epoxy resins are a dominant class of thermoset polymer used in polymer composite materials, which have attractive features of high modulus, strength, and desirable thermal, electrical, and mechanical properties.[5] Currently, commercial epoxy resins are derived from the diglycidyl ether of bisphenol A (DGEBA), an industrial petrochemical which is controversial for its health effects and environmental issues.[6-9] Environmental and sustainability concerns have driven researchers to derive epoxy resins from renewable, non-toxic feedstocks, such as vegetable oils,[10-15] plant sugars,[16] wood alcohol,[17] isosorbide,[18, 19] cardanol,[20, 21] rosin,[22, 23] and lignin.[24-26] However, equally important to the origin of these materials is their end of life behavior.

Polymer degradation under mild conditions is a topic of much interest in polymer science.[27-29] Aliphatic polyesters readily undergo hydrolytic degradation,[30-38] and extensive experimental studies have been undertaken and models developed to describe their degradation

behavior.[39-44] By contrast, the degradation behavior of thermoset polymers has been significantly underexplored. Pyrolysis, also known as thermal degradation, can degrade both DGEBA-based[45-48] and biobased[49-53] epoxy resins, typically requiring temperatures above 400 °C to fully degrade the polymers, and producing low molecular weight byproducts (with little decomposition of the bisphenol A moiety in the case of DGEBA-based resins[45].) Though pyrolysis is an effective way to break down a network polymer, it is also quite energy intensive. Solvolysis can also be employed, in which a chemical reagent reacts with functional groups on the network to decompose it into smaller molecules. DGEBA-based epoxy resins have been depolymerized using nitric acid,[54] tetralin and decalin,[55] CO_2-expanded water,[56] ethanol with $ZnCl_2$,[57] phosphotungstic acid with ethanol,[58] supercritical isopropanol with KOH,[59] alcohol/catalyst systems,[60-64] and near critical water.[65] However, these approaches typically require either chemicals which are not environmentally friendly or high temperatures that are energy intensive. Strategies such as changing the curing agent or incorporating a comonomer can be utilized to minimize the energy needed.[66-68] Photodegradation is generally not a viable option due to its slow kinetics.[69, 70]

Utilizing biorenewable components to replace DGEBA in epoxy resins is an advantageous approach to incorporate functional groups promoting accelerated degradation under benign conditions. Biobased epoxy resins, typically containing ester groups, have been demonstrated to degrade rapidly in acidic solutions in organic solvents or solvent/water mixtures,[71-75] and various factors influence their degradation rate, including solution pH,[71, 74, 75] temperature,[72] degradation time,[72] catalyst concentration,[72] and solvent composition.[74] Even more attractive is to degrade the materials in purely aqueous solutions, without organic solvents. Many biobased epoxy thermosets degrade rapidly in both basic and acidic aqueous solutions,[75-81] showing clear differences in their degradation behavior in acids and bases.[78-81] The rate of degradation depends on choice of epoxy

monomer,[76-79] ratio of epoxy monomer to curing agent,[78, 80, 81] solution pH,[76, 80, 81] and temperature.[80, 81] However, the degradation mechanisms and models for mass loss behavior are still poorly understood in this class of materials.

In this work, we examine hydrolytic degradation behavior of ester-containing biobased epoxy resins in basic solutions, and probe their hydrolytic degradation mechanisms. We explore the degradation behavior of biobased epoxy resins containing high ester content (3 esters per monomer for epoxidized soybean oil and 1 ester per monomer for epoxidized vanillic acid, epoxidized salicylic acid, and epoxidized 4-hydroxybenzoic acid). Importantly, we characterize degradation products following exposure of the resins to basic solutions, identify the degradation mechanism, and quantify degradation rate constants through utilization of solid-state kinetic models.

2. Experimental Methods

2.1. Materials

All chemicals were purchased from Sigma-Aldrich unless otherwise noted and were used as received: ESO was kindly supplied free of charge by Arkema, Inc. (trade name Vikoflex 7170; contains an average of 4.27 epoxide groups per triglyceride molecule following nuclear magnetic resonance, NMR, analysis), vanillic acid (4-hydroxy-3-methoxybenzoic acid, ≥97%), salicylic acid (SA, ≥99%, FG/Halal/Kosher), 4-hydroxybenzoic acid (4HBA, 99%, ReagentPlus), methylhexahydrophthalic anhydride (MHHPA, Huntsman, Aradur HY 1102, ≥99%), 1- methyl-imidazole (1-MI, Huntsman, Accelerator DY 070), N,N-dimethylformamide (DMF, BDH, ≥99.8%, ACS reagent), potassium carbonate (K_2CO_3, ≥99.0%, ACS reagent), allyl bromide (97%), ethyl acetate (BDH, ≥99.5%, ACS grade), magnesium sulfate ($MgSO_4$, BDH, ≥99.0%, anhydrous reagent grade), meta-chloroperoxybenzoic acid (mCPBA, ≤77%), sodium sulfite (Na_2SO_3,

AMRESCO, 98.0%, ACS grade), sodium bicarbonate ($NaHCO_3$, ACS reagent, 99.7-100.3%), hexane (BDH, ≥60%, ACS grade), chloroform (Macron, ACS grade), and silica gel (Macron, grade 62, 60-200 Mesh).

2.2. Preparation of biobased epoxy monomers

Vanillic acid was allylated with the following procedures. Vanillic acid (10.0g, 59.5 mmol) was dissolved into 340 mL of DMF in a 1000 mL round-bottom flask with a magnetic stir bar, sealed with a rubber septum, and cooled to 0 °C using an ice bath. K_2CO_3 (18.1g, 131 mmol) was then added to the flask. After three minutes of stirring, allyl bromide (131 mmol) was added dropwise with a syringe (the molar ratio of ally bromide to vanillic acid was 2.20 to 1, to achieve higher conversion). After adding the allyl bromide, the reaction was allowed to warm to room temperature and the reaction proceeded for 48 h. Distilled water (340 ml) was added to the reactants and the product was extracted by ethyl acetate (three times) in a separatory funnel, by gently shaking the solution for 5 minutes and then allowing it to sit for 1 min; (the product was found in the top layer which was the organic phase). The organic phase was washed with an equivalent volume of saturated brine and dried over $MgSO_4$. Ethyl acetate was removed from the product using a rotary evaporator, and the product was dried in a vacuum oven at 50 °C for 24 h, or until DMF was not observed through NMR analysis. Allylated Vanillic Acid (AVA). ^{1}H NMR (400MHz, chloroform-d, ppm): δ 7.54 (d, J = 9.48 Hz, 1H), 7.46 (d, J = 9.06 Hz, 1H), 7.02 (d, J = 9.28 Hz, 2H), 5.98-6.02 (m, 4H), 5.44-5.38 (m, 2H), 5.26-5.23 (m, 2H), 4.68 (dd, J = 10.54, 2.04 Hz, 2H), 4.54 (dd, J = 9.34, 1.96 Hz, 2H), 3.80 (s, 3H). ^{13}C NMR (100 MHz; chloroform-d, ppm): δ 166.7, 153. 0, 149.6, 133.5, 133.1, 123.9, 123.0, 117.6, 117.4, 112.8, 112.7, 69.8, 65.7, 55.7.

AVA was converted to epoxidized vanillic acid (EVA) through the following procedures. AVA (5.00g, 20.1 mmol) was dissolved into 500 mL chloroform in a 1000 mL glass round bottom

flask with a magnetic stir bar sealed with a rubber septum. mCPBA (27.8g, 161 mmol) was added to the flask (at a molar ratio of allylated vanillic acid : mCPBA of 8 : 1). The solution was stirred at 40 °C for 24 hours. After 24 hours, the solution was washed with an equivalent volume of a 10%wt Na_2SO_3 aqueous solution and separated using a separatory funnel. The organic phase (bottom layer) was then washed with an equivalent volume of a saturated $NaHCO_3$ solution and separated using a separatory funnel. Finally, the organic phase (bottom layer) was washed with an equivalent volume of saturated brine and separated using a separatory funnel. The chloroform was then removed from the product using a rotary evaporator. The EVA product was purified by silica gel chromatography using hexane/ethyl acetate (40/60). The organic solvent was removed using a rotary evaporator and the product was dried in a vacuum oven at 60 °C overnight. Epoxidized Vanillic Acid (EVA). ^{1}H NMR (400MHz, chloroform-d, ppm): δ 7.66 (d, J = 9.28 Hz, 1H), 7.52 (d, J = 9.08 Hz, 1H), 6.94 (d, J = 9.24 Hz, 2H), 4.64 (dd, J = 13.28, 3.04 Hz, 1H), 4.36 (dd, J = 12.34, 2.96 Hz, 1H), 4.13-4.10 (m, 1H), 4.09-4.05 (m, 1H), 3.96 (s, 3H), 3.45 (dd, J = 9.48, 9.48 Hz 1H), 3.42 (dd, J = 9.56, 9.56 Hz, 1H), 2.96-2.92 (m, 2H), 2.82-2.77 (m, 2H). ^{13}C NMR (100 MHz; chloroform-d, ppm): δ 166.7, 153. 2, 149.0, 123.2, 123.0, 113.3, 113.1, 69.2, 65.8, 50.2, 49.9, 45.1, 45.0.

Epoxidized salicylic acid (ESA) and epoxidized 4-hydroxybenzoic acid (E4HBA) were synthesized following previously reported procedures.[82]

2.3. Preparation of epoxy resins

EVA was melted at 94 °C prior to use (the other epoxy monomers were liquids at room temperature). The epoxy monomer (DGEBA, ESO, EVA, ESA, or E4HBA) was mixed with MHHPA (stoichiometry based on equal molar epoxide and anhydride groups) and 3 phr (parts per

hundred parts by weight of resin) 1-MI at 50 °C in a 20 mL scintillation vial using magnetic stirring for 10 minutes. The mixture was placed in the following sample holders appropriate for each characterization experiment: (a) in a preweighed Tzero aluminum pan for differential scanning calorimetry, (b) in a pan for thermogravimetric analysis, and (c) in an aluminum mold for hydrolysis degradation analysis. The sample was then transferred to a convection oven and cured. The following curing schedule was used for EVA, ESA, E4HBA, and DGEBA-based epoxy resins: 70 °C for 2 hours, then 170 °C for 2 hours. ESO required a longer first curing stage (as the reaction kinetics were significantly slower), with the following curing schedule: 70 °C for 24 hours, then 170 °C for 2 hours. Table 1 shows the amount of epoxy monomer, curing agent, and catalyst used for each sample.

Table 1: Amounts of epoxy monomer, curing agent and catalyst used in epoxy resin synthesis

Epoxy Monomer	Epoxy Monomer Mass (g)	Curing agent Mass (g)	Catalyst Mass (g)
DGEBA	1	0.97	0.03
ESO	1	0.75	0.03
EVA	1	1.20	0.03
ESA	1	1.35	0.03
E4HBA	1	1.35	0.03

2.4. Nuclear Magnetic Resonance

^{1}H NMR (400, 500, 600 MHz) and ^{13}C NMR (100 MHz) experiments were conducted using a JEOL ECA-400 instrument with deuterated chloroform (Cambridge Isotope Laboratories, Inc., 99.8 atom % D) as the solvent. Chemical shifts were referenced to the solvent proton resonance (7.26 ppm for ^{1}H NMR, 77.2 ppm for ^{13}C NMR).

2.5. Differential Scanning Calorimetry

Differential scanning calorimetry (DSC) was conducted with a TA Instruments Q2000 differential scanning calorimeter, under 50 ml/min nitrogen flow, and calibrated with an indium standard. Samples were encapsulated in a Tzero aluminum pan, equilibrated at 40 °C, and subjected to a heat-cool-heat cycle from 40 –200 °C at a rate of 10 °C/min. The glass transition (T_g) was identified as the inflection point in the second heating cycle.

2.6. Thermogravimetric Analysis

Thermogravimetric analysis (TGA) experiments were conducted using a TA Instruments Q500 analyzer. The samples were heated from 25 °C to 550 °C at a rate of 10 °C/min in an argon environment.

2.7. Optical Microscopy

Optical microscopy was performed on a Leica DM2500 M microscope with a HCX PL FLUOTAR 20X/0.50 BD objective in bright field mode using a mercury lamp. Optical microscopy slides were prepared by taking a drop of reactive monomer mixture, sandwiching it between a glass slide and a glass coverslip, and curing the epoxy resin following the protocol described previously. For optical micrographs which showed dispersed particles, the micrographs were converted to binary images, and processed with ImageJ to identify the pixel area for each particle. With knowledge of the microns/pixel of the micrograph, each particle area in micron^2 was characterized. Assuming a circular particle, the circle diameter was calculated ($D_i = 2(A_i/\pi)^{1/2}$). We did not account for the potential underestimation of D_i due to the two dimensional projection of the sphere. Additionally, particles of a size too small to be observed at the magnification chosen

have been neglected. The Sauter mean diameter (D_m) was calculated for the population of oil droplets in the micrograph (equation 1):

$$D_m = \frac{\sum_i^n {D_i}^3}{\sum_i^n {D_i}^2}, \quad (1)$$

where D_i is the diameter of one particle and n is the number of particles in 1 micrograph. The standard deviation was calculated based on the population of particles examined within the same image. In the case where co-continuous morphologies were observed, optical micrographs were processed using the ImageJ Fast Fourier transform (FFT) function. The average domain size (d) was taken to be that at the peak maximum in the intensity versus wavevector ($q=2\pi/d$). The error was quantified by calculating the peak width at half maximum.

2.8. Scanning Electron Microscopy

The surface structures of the neat and degraded samples were imaged using a Jeol JSM-6010LA field emission scanning electron microscope at a voltage of 15kV. The surface was etched with ionized argon gas and subsequently coated with gold using a Denton Vacuum Desk V sputter coater for 1.5 minutes. The gold thickness was approximately 10 nm.

2.9. Mass Spectrometry

Mass Spectrometry experiments were conducted using a Bruker MicroToF ESI LC-MS System. This MicroToF instrument is equipped with an ESI source and is interfaced with an Agilent 1200 HPLC system. The mobile phase was a mixture of 50% water and 50% ethanol. The epoxy resin degradation products were dissolved in acetonitrile and the concentration of the solution was 10 μg/ml prior to injection into the MicroToF.

2.10. Fourier Transform Infrared Spectroscopy

FTIR spectra were obtained on a Thermo Scientific Nicolet 4700 spectrometer in transmission mode. The OMNIC Series software was used to follow selected peaks at 1.928 cm^{-1} resolution using 32 scans.

2.11. Contact Angle Measurements

Water contact angles were measured using an OCA 15EC video-based optical contact angle measuring instrument at ambient temperature. The SCA 20 software was used to record the water contact images. 1μL DI water droplets were deposited onto 5 different positions on polished surfaces of the epoxy resins. 1500 grit sandpaper was used to polish the sample surfaces and dust was removed using compressed nitrogen.

2.12. Hydrolytic Degradation Experiments

Epoxy resin samples (10mm × 5mm ×3mm) were degraded in basic solutions following literature procedures.[76, 83] The initial sample weight was recorded, and the sample was placed in 10 mL of 3 wt% NaOH solution at 80 °C for a specified time period (0.04 wt% sodium azide was also added to the solution to prevent microbial growth). The sample was then rinsed with deionized (DI) water, rinsed with a 1 wt% HCl solution to neutralize the solution, rinsed with DI water again, and finally dried in a vacuum oven at 50 °C overnight. The sample weight was recorded, and then the sample was placed back in the NaOH solution for additional time. This process was repeated until the whole sample degraded.

3. Results and Discussion

3.1. Epoxy monomer synthesis and epoxy resin curing protocol

A variety of biobased epoxy monomers, which contain ester groups, were prepared (Figure 1). Vanillic acid, derived from lignin,[84, 85] was converted to epoxidized vanillic acid (EVA). Plant-based phenolic acids, salicylic acid and 4-hydroxybenzoic acid, were converted to epoxidized salicylic acid (ESA) and epoxidized 4-hydroxybenzoic acid (E4HBA), respectively. Epoxidized soybean oil (ESO) was obtained from a commercial source.

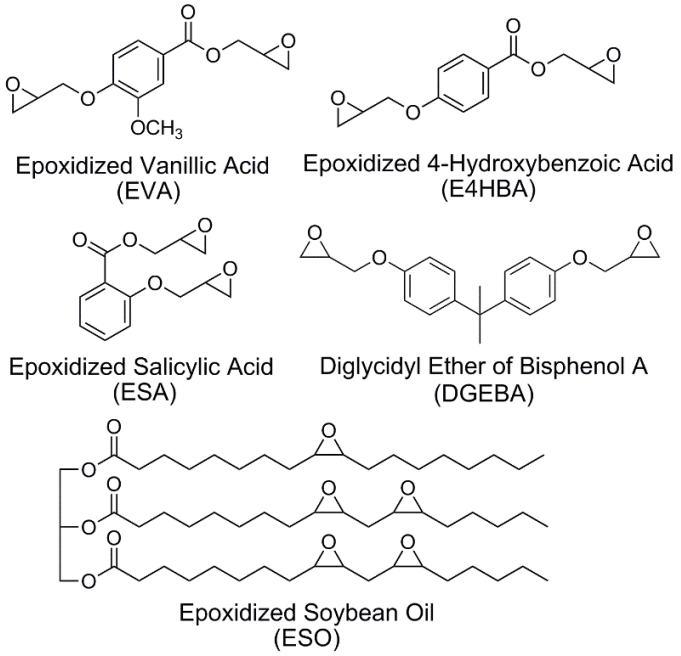

Figure 1: Chemical structures of epoxidized vanillic acid (EVA), epoxidized salicylic acid (ESA), epoxidized 4-hydroxybenzoic acid (E4HBA), epoxidized soybean oil (ESO), and diglycidyl ether of bisphenol A (DGEBA), used in this study.

A two-step procedure was employed for the synthesis of EVA (Scheme 1). This procedure, based on literature,[86] was previously reported by our group for the synthesis of ESA and E4HBA,[82] and avoids the toxicity concerns of the use of epichlorohydrin. Briefly, vanillic acid was reacted with allyl bromide to form allylated vanillic acid (AVA), which was subsequently reacted with

mCPBA to form EVA (Scheme 1). An alternative one-step synthetic protocol for the preparation of EVA has been previously reported.[84]

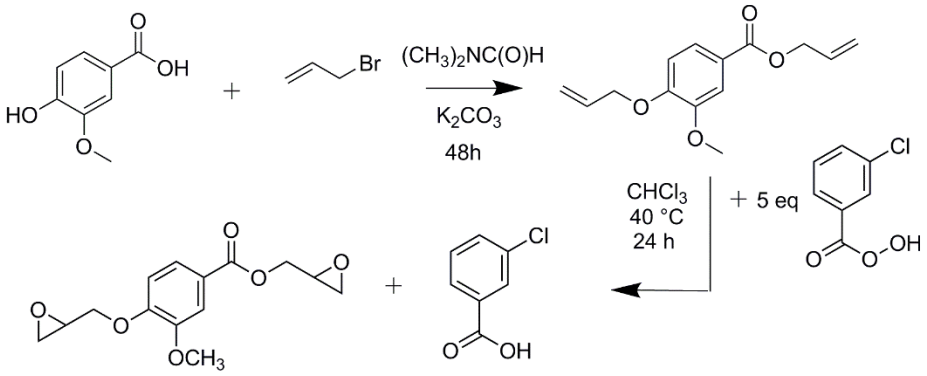

Scheme 1: Synthesis of EVA.

^{1}H NMR analysis identified the structures of AVA and EVA (Figure 2; vanillic acid spectra shown in Figure S1 for reference). The peaks in the region of 5-6 ppm are associated with the allyl groups in AVA. The disappearance of the allyl group peaks at 5-6 ppm, and presence of epoxide peaks in the region of 2.5-3.5 ppm, confirmed the conversion of allyl groups to epoxide groups in EVA. The AVA and EVA structures were further confirmed with ^{13}C NMR analysis (Figure S2).

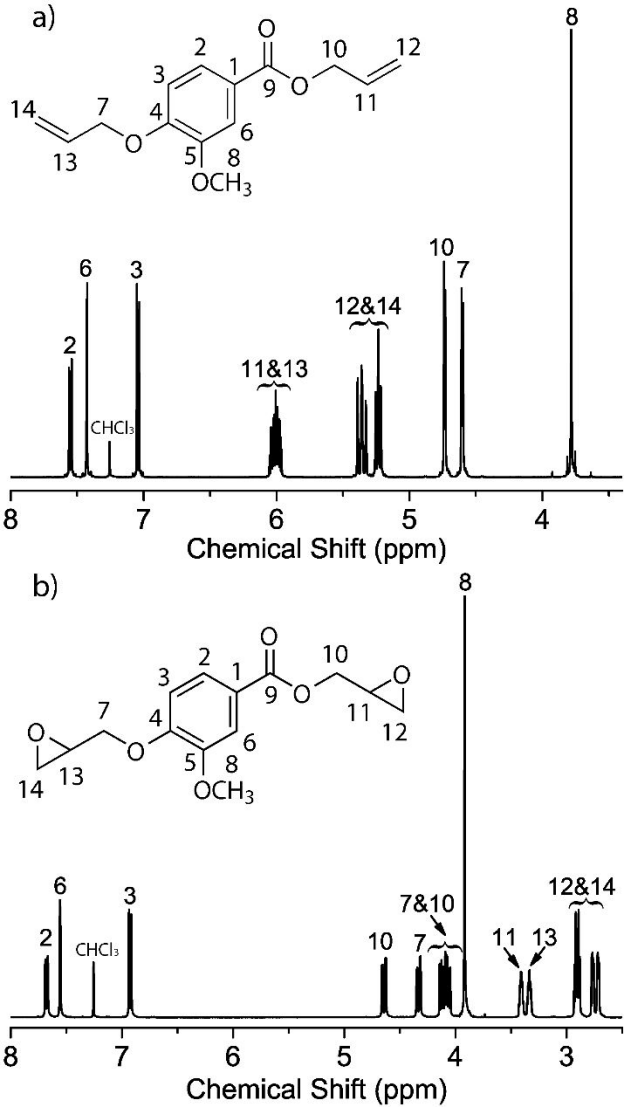

Figure 2: ^{1}H NMR spectra of a) AVA and b) EVA. The conversion and yield of the allylation of vanillic acid to form AVA were 99% and 98%, respectively. The conversion and yield of the epoxidation of AVA to form EVA were 70% and 32%, respectively.

The epoxy monomers (EVA, ESA, E4HBA, ESO and DGEBA) were cured with a curing agent to form highly crosslinked epoxy resin thermosets. Following our prior work on the preparation of epoxy resins from ESA and E4HBA, we employed an anhydride curing agent (MHHPA) along with a catalyst (1-MI),[82] shown in Figure 3. Previously, we demonstrated this curing agent produced biobased epoxy resins (using ESA and E4HBA monomers) with desirable thermal and mechanical properties.[82]

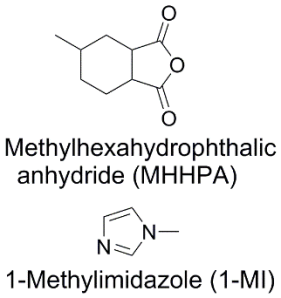

Figure 3: Curing agent and catalyst used in this study.

The curing of the epoxy monomers with MHHPA/1-MI (Schemes S1-S5) was investigated with *in situ* DSC analysis. EVA was melted first at 94 °C (as its onset melting temperature was 91 °C, Figure S3) before adding the stoichiometric amount of curing agent and 1-MI catalyst and mixing them at 50 °C. The ESA, E4HBA, ESO, and DGEBA monomers were mixed with stoichiometric amounts of curing agent and 1-MI catalyst at 50 °C. The mixtures of epoxy monomer/MHHPA/1-MI were then sealed in DSC pans and monitored with DSC while heating at a constant rate of 10 ° C/min. The resulting DSC data are shown in Figure 4. While EVA, ESA, and E4HBA exhibited similar curing temperatures under constant heating rate to that of DGEBA, the ESO monomer required significantly higher temperature for complete curing. The higher curing temperature of the ESO-based epoxy resin is attributed to the presence of less accessible internal epoxide groups; in contrast, DGEBA, EVA, ESA, E4HBA contain terminal epoxy groups.[87, 88]

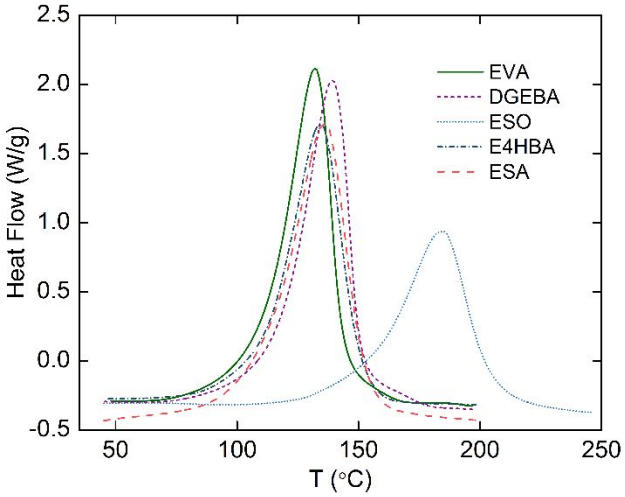

Figure 4: *In situ* DSC data obtained upon curing EVA, ESA, E4HBA, ESO, and DGEBA monomers with MHHPA (catalyzed with 1-MI). (Data for ESA and E4HBA monomers were obtained from ref. [82]).

We employed a two-stage curing protocol for all of the epoxy resins, following our prior work.[82] The first, lower temperature, curing stage was used to promote curing without evaporation of monomer or curing agent. The second, higher temperature, curing stage was selected well above the T_g of the cured resin to avoid vitrification and maximize reaction conversion. The onset evaporation temperatures for the epoxy monomers were identified from TGA as 275 °C (EVA), 90 °C (ESA),[82] and 97 °C (E4HBA),[82] and that of the MHHPA curing agent was 95 °C (Figures S3-S4). To avoid monomer evaporation, the first curing stage was conducted at 70 °C. After mixing the reactants and stirring at 50 °C for 10 minutes until the solution became transparent, the mixture was placed in a convection oven at 70 °C for various time periods until the mixture visually solidified (requiring 2 h of curing at 70 °C for EVA, ESA, E4HBA, and DGEBA, and 24 h of curing at 70 °C for ESO). The temperature of the second curing stage was set at 170 °C, well above the T_g of the cured epoxy resins. To identify the time of the second curing stage, T_g was monitored as a function of second stage curing time (Figure S5). For all epoxy resins, an optimal second stage curing time was determined to be 2 h, allowing for maximum conversion, providing consistently

high T_g values (with little deviation), and avoiding thermal degradation (Figure S5). The resulting EVA-based epoxy resin exhibited a high T_g (146 ± 2 °C), comparable to that of the traditional DGEBA-based epoxy resin (140.1 ± 0.4 °C) and slightly higher than that of the ESA- and E4HBA-based epoxy resins (131 ± 3 °C and 136 ± 5 °C, respectively[82]). The ESO-based epoxy resin exhibited a significantly lower T_g (69 ± 7 °C).

3.2. Thermal properties and phase behavior of epoxy resins prepared from mixtures of ESO and DGEBA.

Mixtures of DGEBA and ESO monomers, with contents varying from 0-100 wt% ESO (of the total ESO and DGEBA content), were cured with a stoichiometric amount of MHHPA (catalyzed with 1-MI). The resulting epoxy resin T_g as a function of ESO content is shown in Table 2. Increasing the ESO content resulted in a substantial decrease in T_g. In addition, epoxy resins with higher ESO content exhibited larger deviations in the T_g. Optical microscopy was used to test the phase homogeneity of the epoxy resins (Figures 5 and S6). The background subtracted images indicated that the epoxy resins containing 40, 60 and 80% ESO (relative to the total amount of ESO and DGEBA) were macroscopically phase separated into ESO-rich and DGEBA-rich domains (both prior to and after the second curing stage), whereas the epoxy resin with 20 wt% ESO was homogeneous throughout the curing process. As DGEBA and ESO have disparate curing kinetics (Figure 4), it is likely that the more rapid curing of the DGEBA monomer promotes phase separation of the DGEBA-rich domains from the unreacted ESO. The epoxy resin containing 40 wt% ESO exhibited a submicron average particle size of 0.6 μm (Table 2). A drastic increase in particle size was observed for the epoxy resins with 60 and 80 wt% ESO (9.4 and 9.8 μm, respectively). The morphology was also distinct for the three epoxy resins: the sample with 40 wt% ESO exhibited a co-continuous morphology whereas the 60 and 80 wt% samples exhibited

dispersed particle morphologies, in which the particles aggregated into strands in the 80 wt% sample.

Table 2: T_g and domain size for epoxy resins prepared from mixtures of ESO and DGEBA cured with MHHPA/1-MI.

Monomer[a]	T_g (°C)	Domain size (μm)
0% ESO	140.1 ± 0.4	NA[b]
20% ESO	120 + 2	NA[b]
40% ESO	117 ± 2	0.6 ± 0.1[c]
60% ESO	103 ± 1	9.4 ± 0.4[d]
80% ESO	90 ± 6	9.8 ± 0.4[d]
100% ESO	69 ± 7	NA[b]

[a] wt% ESO indicates ESO content relative to total amount of ESO and DGEBA
[b] Homogeneous samples
[c] Characterized from FFT of the optical micrograph (domain size = 2π/q)
[d] Sauter-mean diameter of the dispersed particles (Equation 1). Particle size distributions shown in Figure S7.

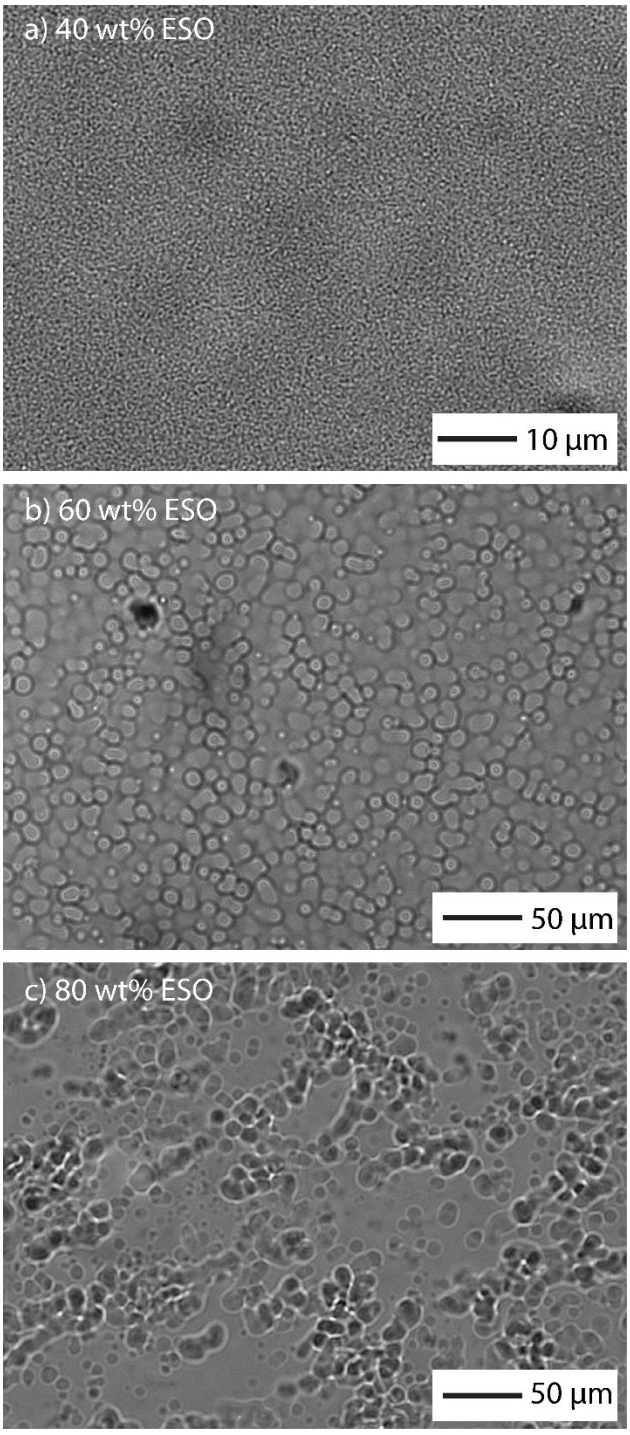

Figure 5: Optical microscopy images of epoxy resins with differing ESO content (wt% ESO is the ESO content relative to the total amount of ESO and DGEBA).

3.3. Degradation behavior of biobased epoxy resins

The hydrolytic degradation behavior of the epoxy resins was characterized by placing the samples in 3 wt% NaOH solution at 80 °C and monitoring their mass as a function of exposure time in the basic solution (Figure 6). All biobased epoxy resins, in which the epoxy monomers contain ester groups, exhibited significantly more rapid degradation rates relative to the DGEBA-based epoxy resin (Figure 6a). The anhydride-cured ESO-based epoxy resin exhibited the fastest degradation rate (disappearing within 4-5 days, Figure 6a). While the curing of an epoxy monomer with an anhydride curing agent produces a small concentration of esters throughout the epoxy network, amine-curing does not have this affect. The anhydride-cured ESO-based epoxy resin exhibited a slightly faster degradation rate than that of the amine-cured ESO-based epoxy resin reported previously by our group.[76] The rapid degradation behavior of the ESO-based epoxy resin is in stark contrast to the behavior of the DGEBA-based epoxy resin: with anhydride-curing, the DGEBA-based epoxy resin showed a slow degradation rate (Figure 6), and with amine-curing, it did not exhibit any noticeable mass loss in the basic solution, for up to 3 months.[76] The ESA-based epoxy resin also rapidly degraded, at a rate slightly slower than that of the ESO-based epoxy resin. E4HBA- and EVA-based epoxy resins exhibited more moderate degradation rates (Figure 6a). We also probed the degradation behavior of epoxy resins synthesized from mixtures of ESO and DGEBA monomers, in which the degradation rate was tunable based upon the relative concentration of ESO in the epoxy resin. The degradation rate systemically increased with increasing ESO content in the epoxy resin (Figures 6b and 6c). Camera images of the epoxy resins at different degradation times are shown in Figure 7.

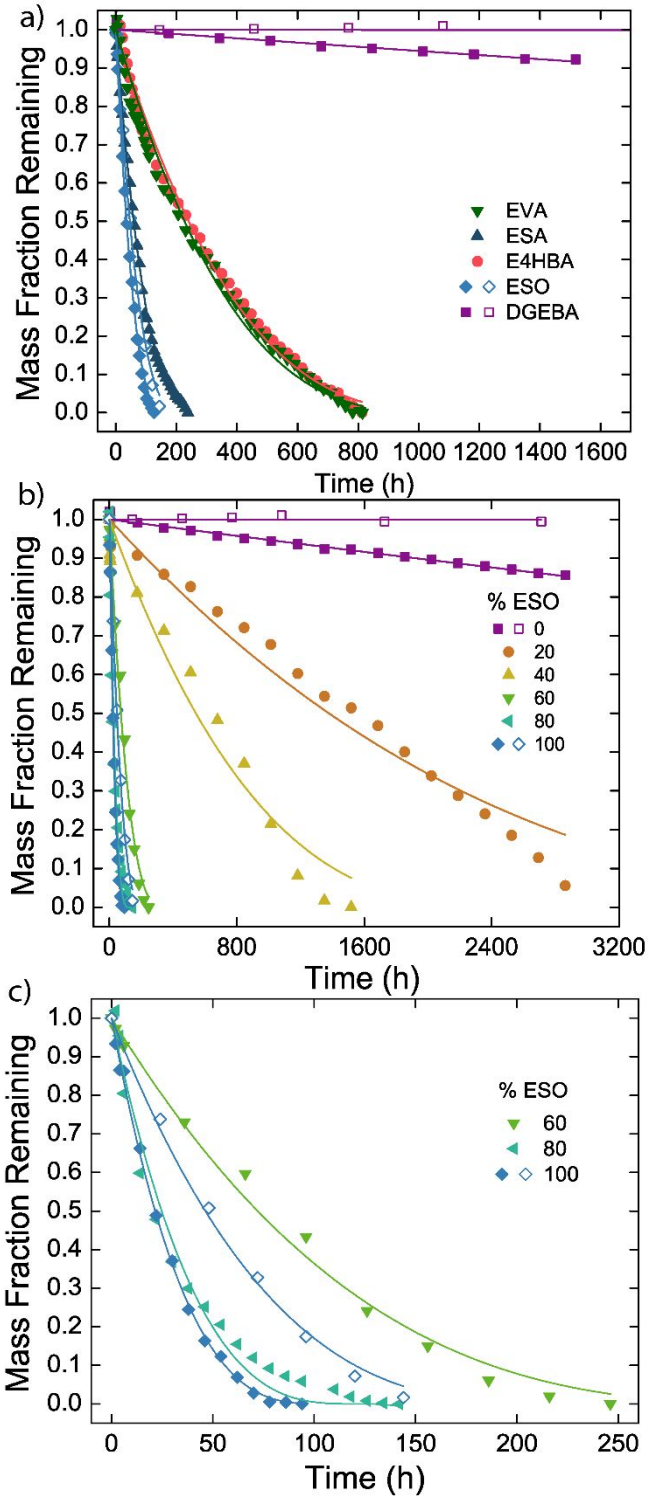

Figure 6: Fraction of mass remaining of epoxy resins as a function of exposure time in a 3 wt% NaOH solution at 80 °C for: a) EVA, ESA, E4HBA, ESO and DGEBA-based epoxy resins; and

b) c) epoxy resins prepared from mixtures of ESO/DGEBA with varying ESO content (relative to total amount of ESO and DGEBA). Solid symbols indicate anhydride-cured epoxy resins, whereas open symbols indicate amine-cured epoxy resins (data on amine-cured epoxy resins was obtained from ref.[76]). Solid curves indicate fits with the contracting volume model. For E4HBA and EVA-based epoxy resins, only one data point for every three collected is shown in the plot for clarity.

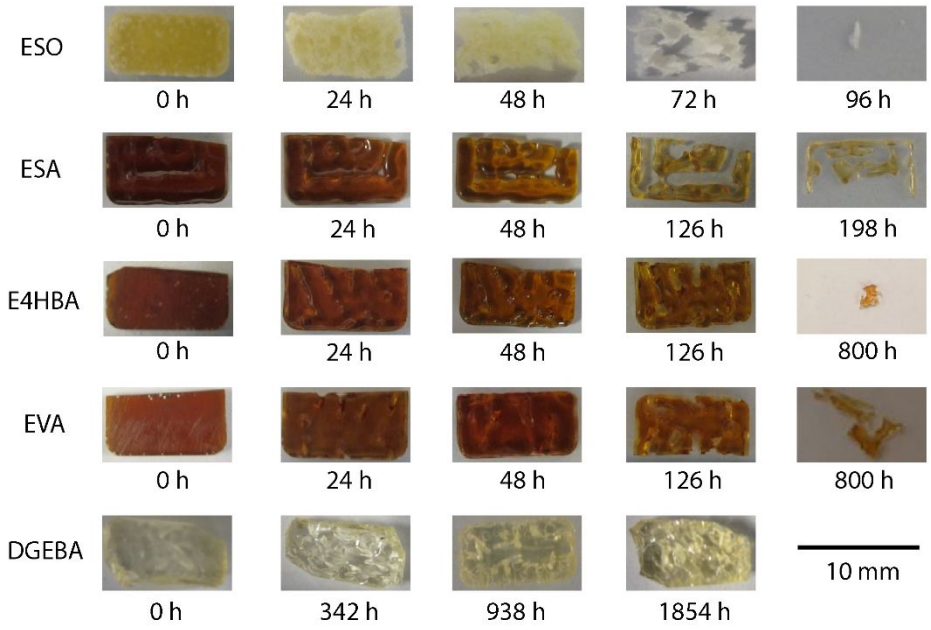

Figure 7: Camera images of epoxy resin specimens following exposure to a 3wt% NaOH solution at 80 °C.

3.4. Exploration of a model for ester-containing thermoset degradation

It is well established that linear polyesters undergo significantly different degradation behaviors in basic and acidic solutions.[36, 89] Polyesters degrade through two primary mechanisms: bulk and surface erosion,[41] which occur in acidic and basic solutions, respectively.[30, 31] In bulk

erosion, hydrolysis occurs throughout the entire specimen simultaneously, whereas in surface erosion, hydrolysis mainly occurs in the region near the surface. The hydrolysis mechanisms of linear polyesters such as polylactide and poly(lactide-*co*-glycolide) have been described with well-established models,[90-92] but few studies have examined the degradation behavior of crosslinked thermosets containing ester groups. We therefore hypothesized that epoxy thermosets containing ester groups would also follow the surface erosion mechanism in basic solutions.

The contracting volume model describes the dissolution of a cubic solid governed by contraction of the sample volume as the solid-liquid interface moves toward the specimen center.[93] In application of this model, the rate limiting step in the erosion of the sample is assumed to be contraction of the solid-liquid interface, rather than nucleation, diffusion, or even the chemical reaction which occurs at the surface. A prior literature study has successfully applied this model to the catalyzed solvolysis of a DGEBA-based epoxy resin at elevated temperatures.[63] We have extended this model to the rectangular cuboid-shaped degradation samples employed in this study (described in the *ESI*) (equation 2):

$$1 - (1 - \alpha)^{1/3} = kt \qquad (2)$$

where α is the mass fraction of the sample remaining at time t, and k is the degradation rate constant. The contracting volume model was applied to mass loss data obtained from the biobased epoxy resins in 3 wt% NaOH solution at 80 °C (solid curves in Figure 6). The model described the degradation profile well for all the neat epoxy resins (with R^2 values of 0.985 to 0.998 (Figure 6a)). We considered other solid-state kinetic models, such as n^{th} order reaction models, diffusion-based models, and nucleation-based models, but these models provided a worse fit to the data (Figure S10 and Table S2). There were larger deviations between the model and data for epoxy

resins synthesized from mixtures of ESO and DGEBA with lower ESO content (20-40 wt% ESO, with R^2 values ranging from 0.950 to 0.958). There may be some influence of the presence of macroscopically phase separated ESO-rich and DGEBA-rich domains (i.e. Figure 5) on the degradation rate. Additionally, the ESO segments of the network may not be uniformly distributed throughout the network, which could influence the observed degradation rate.

The fitted rate constants (k) for all the epoxy resins are listed in Tables 3 and 4. The ESO-based epoxy resin (with the highest concentration of esters in the epoxy network - 3 esters per ESO monomer) exhibited the largest degradation rate constant k, followed by the ESA-based epoxy resin. Interestingly, though the ESA and E4HBA monomers contain the same number of ester groups (1 per monomer), and differ only in the placement of the ester groups along the aromatic ring (*ortho* vs. *para* placement, respectively), the E4HBA-based epoxy resin showed a more moderate degradation rate constant than that of the ESA-based epoxy resin. EVA- and E4HBA-based epoxy resins, which contain the same *para* placement of ester groups on the epoxy monomer and differ only in the addition of a methoxy group to the EVA monomer, exhibited indistinguishable degradation rate constants. Finally, the DGEGA-based epoxy resin, for which the DGEBA monomer does not contain any ester groups, exhibited a significantly smaller degradation rate constant as compared to all biobased epoxy resins. The rate constant for epoxy resins synthesized from mixtures of DGEBA and ESO increased systematically with increasing ESO content in the resin (Table 4).

Table 3: Degradation rate constant, k (in a 3 wt% NaOH solution at 80 °C) and physical properties of epoxy resins cured with MHHPA/1-MI.

Monomer	k ($\times 10^{-3}$ mm^{-1} hr^{-1})	T_g (°C)	Water Contact Angle (°)	# of esters in epoxy monomer
ESO	8.4 ± 0.9	69 ± 7	53 ± 2	3
ESA	2.9 ± 0.6	131 ± 3	59 ± 1	1
E4HBA	0.8 ± 0.3	136 ± 5	61 ± 2	1
EVA	0.8 ± 0.1	146 ± 2	58 ± 3	1
DGEBA	0.02 ± 0.01	140.1 ± 0.4	65 ± 1	0

Table 4: Degradation rate constant, k (in a 3 wt% NaOH solution at 80 °C) for epoxy resins prepared from mixtures of ESO and DGEBA cured with MHHPA/1-MI.

Monomer[a]	k ($\times 10^{-3}$ mm^{-1} hr^{-1})
0% ESO	0.02 ± 0.01
20% ESO	0.17 ± 0.02
40% ESO	0.44 ± 0.02
60% ESO	2.9 ± 0.1
80% ESO	9.0 ± 0.7
100% ESO	8.4 ± 0.9

[a] wt% ESO indicates ESO content relative to total amount of ESO and DGEBA

3.5. Investigation of the degradation mechanisms in ester-containing thermosets

SEM was used to further confirm the surface erosion mechanism of the epoxy resins in basic solutions. The surfaces of neat ESO and DGEBA-based epoxy resins, as well as those degraded in basic solutions for 6 and 50 h, were observed with SEM (Figure 8). Both neat samples had homogeneous and flat surfaces. After 6 h in basic solution, the ESO-based epoxy resin exhibited various-sized crevices in the surface, whereas the DGEBA-based epoxy resin exhibited only minor scratches. As the degradation time increased, both the crevices on the ESO-based epoxy resin and the scratches on the DGEBA-based epoxy resin surfaces grew, an indication of

surface erosion. The crevices on the surface of the ESO-based epoxy resin likely provided pathways for more regions of the sample to be exposed to the solution.

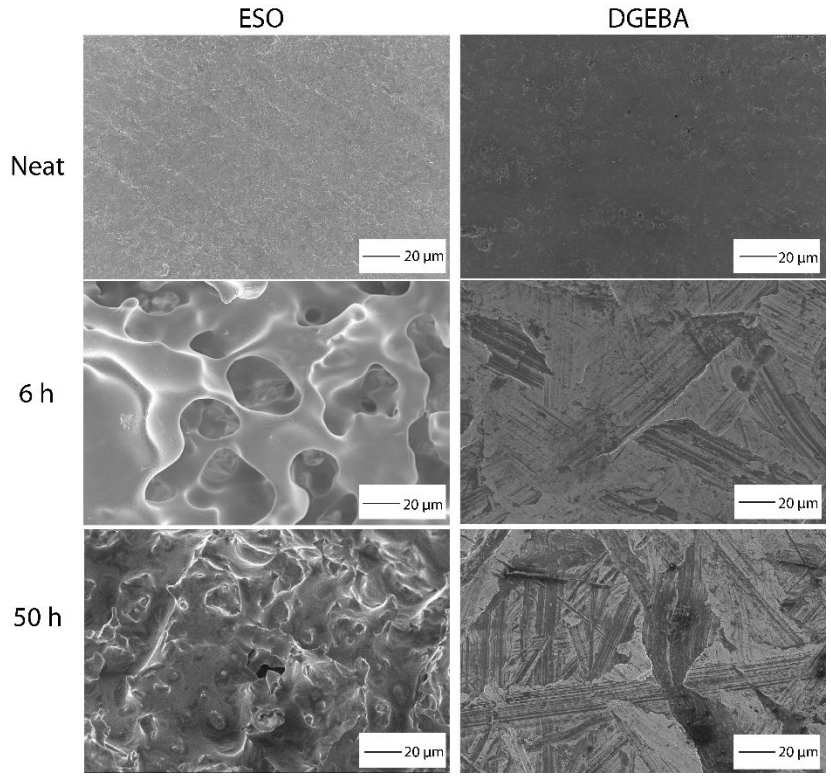

Figure 8: SEM images of the surfaces of ESO-based and DGEBA-based epoxy resins, showing surface changes after soaking in a 3wt% NaOH solution at 80 °C for 6 and 50 h. (Lower magnification images are shown in Figure S8).

Mass spectrometry was used to investigate the degradation mechanism (Figures 9 and S9). We fully degraded the ESO-based epoxy resin and removed all the solvent. The degradation products were then dissolved in acetonitrile, at a concentration of 10 µg/ml. Soybean oil is comprised of a mixture of fatty acids,[94] mainly oleic acid, linoleic acid, linolenic acid, and smaller contents of stearic acid and palmitic acid. Therefore, the ESO monomer may contain any combination of these fatty acids, in which unsaturated carbon-carbon double bonds have been converted to epoxide groups. We considered all possibilities for the ESO monomer chemical

structure (detailed description in the *ESI*). We also considered that in addition to the esters present on the ESO monomer, anhydride curing may result in ester formation. The spacing of isotope peaks on the mass spectrum indicated that all molecules had single charges. With this information, we calculated the m/z values of each of the possible chemical fragments that could remain after cleavage of the ester groups on the epoxy resin network through ester hydrolysis (Scheme 2). We also considered the presence of either H^+ or Na^+ ions, and the possibility of exchange between H and Na within the molecules (Na was likely present due to the use of NaOH for the degradation process). Mass spectrometry peaks with intensities below 500 were neglected, as this is commensurate with the background intensity.

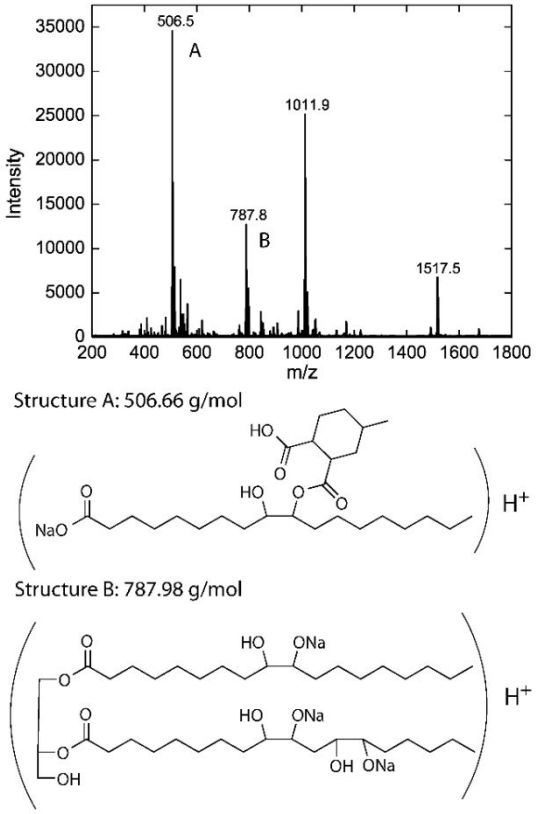

Figure 9: Mass spectrometry analysis of degradation products of the ESO-based epoxy resin. The peaks labeled A and B are associated with the structures indicated below the data. The additional peaks at 1011.9 and 1517.5 m/z are likely aggregates of 2 or 3 molecules with structure A, respectively. (Closer view of mass spectrometry data in Figure S9).

There were four main components in the degradation products, whose m/z values were 506.5, 787.8, 1011.9 and 1517.5. The peaks located at 506.5 and 787.8 are consistent with the two degradation products whose molecular structures are shown as A and B in Figure 9. Aggregates of two or three molecules with structure A are consistent with the peaks observed at 1011.9 and 1517.5 m/z, respectively. The presence of these major degradation products further confirmed that mechanism of the degradation was the hydrolysis of the ester groups. Other minor peaks present in the spectrum were also investigated and the structures are shown in Table S1.

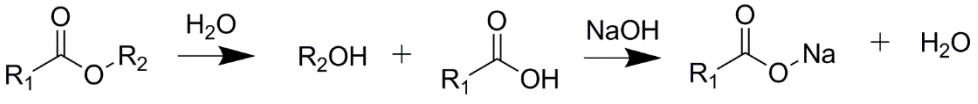

Scheme 2: Epoxy resin degradation through ester hydrolysis (with neutralization reaction).

3.6. Additional factors influencing epoxy resin degradation

Many factors may potentially influence the degradation rates of epoxy resins in basic solution (Table 3). As degradation proceeds as the hydrolysis of ester groups, we hypothesize that the number of ester groups per monomer should have a large influence on the degradation rate. The slowest-degrading epoxy resin, DGEBA, contains 0 ester groups per monomer, while the fastest-degrading epoxy resin, ESO, contains 3 ester groups per monomer. ESA, E4HBA, and EVA contain 1 ester per monomer, and exhibited intermediate degradation rates as compared to DGEBA and ESO. However, we also anticipate that the hydrophilicity of the epoxy resin surface plays an important role in the surface erosion process.[80, 81, 95] We measured the water contact angle on the epoxy resin surfaces, and found that the ESO-based epoxy resin was the most hydrophilic, whereas the DGEBA-based epoxy resin was the most hydrophobic (Table 3). Additionally, we may consider proximity to the T_g

and crosslink density as factors that may influence the degradation rate.[80, 81, 95] The ESO-based epoxy resin exhibited a significantly reduced T_g as compared to the other epoxy resins (Table 3), and the low T_g also suggests the crosslink density of the ESO-based epoxy resin is significantly lower than that of the other epoxy resins.[96] The low T_g (below the temperature at which sample degradation was conducted) and reduced crosslink density may have accelerated the degradation of the ESO-based epoxy resin. By contrast, the biobased epoxy resins containing aromatic groups (ESA, E4HBA, and EVA) all exhibited similar T_g's, and likely similar crosslink densities, as compared to the DGEBA-based epoxy resin (Table 3). Thus, the accelerated degradation rates of these biobased epoxy resins as compared to the DGEBA-based epoxy resin is likely due to their increased ester content and higher degree of hydrophilicity.

In summary, this work extends the existing knowledge of thermoset degradation behavior, showing biobased epoxy resins with higher ester contents undergo rapid degradation under mild conditions (low temperatures and thus low energy requirements, and in aqueous solutions). As hydrolytic degradation is an important aspect of polymer biodegradation, these results may be extended to create biodegradable thermoset polymers, which can be processed at the end of their life in a compost environment, providing new thermoset waste treatment options.

Conclusions

We investigated the accelerated hydrolytic degradation of epoxy resins in a basic solution at 80 °C, including a new epoxy resin derived from vanillic acid (a lignin-derived molecule), as well as epoxy resins derived from plant-based phenolic acids, soybean oil, and bisphenol A (the conventional epoxy monomer source). The biobased epoxy resins (excluding the vegetable oil-

based resins) exhibited glass transition temperatures comparable to that of the conventional epoxy resin. The biobased epoxy resins all exhibited more rapid hydrolytic degradation behavior due to higher ester content and higher degree of hydrophilicity, in contrast to the conventional DGEBA-based epoxy resin. The degradation rate of the ESO-based epoxy resin was further enhanced by reduced glass transition temperature and crosslink density. A solid-state kinetic model was used to model the degradation behavior, which was in good agreement with experimental data for the neat epoxy resins. The ESO-based epoxy resin (containing 3 esters per monomer) exhibited the largest degradation rate constant k, followed by the ESA-based epoxy resin (1 ester per monomer, *ortho* placement of ester groups). EVA- and E4HBA-based epoxy resins (1 ester per monomer, *para* placement of ester groups) exhibited more moderate, and indistinguishable, degradation rate constants. Finally, the DGEBA-based epoxy resin (no esters per monomer) exhibited a significantly smaller degradation rate constant as compared to all biobased epoxy resins. Epoxy resins derived from mixtures of ESO and DGEBA showed tunable degradation rate constants, systematically increasing as the ESO wt% constant was increased. The degradation mechanism was explored and confirmed as surface erosion. Mass spectrometry analysis verified degradation proceeded through hydrolysis of ester groups. These results demonstrate biobased epoxy resins with higher ester contents and higher degree of hydrophilicity can be hydrolytically degraded more rapidly than conventional epoxy resins, and under mild conditions (low temperatures, and in aqueous solutions), which could be leveraged for the creation of biodegradable thermoset polymers.

Conflicts of interest

The authors declare no competing financial interests.

Acknowledgements

We are grateful to the financial support from the National Science Foundation (CMMI-1334838, DMR-1611376, and DMR-1460564) and Norman Hackerman Advanced Research Program of the Texas Higher Education Coordinating Board (003652-0022-2013). The authors would like to thank Ramanan Krishnamoorti, Wenyue Ding, Jialin Qiu and Xuejian Chen for access, training, and data analysis on the FTIR and TGA instruments. We appreciate the assistance of Scott K. Smith for access and training in the University of Houston Department of Chemistry Nuclear Magnetic Resonance Facility. We thank Navjot Singh Randhawa for access and training on the scanning electron microscope and gold sputter in the University of Houston Cullen College of Engineering Microscopy Center. We thank the Rice University Shared Equipment Authority for access to the Bruker MicroToF ESI LC-MS system. We thank Jacinta Conrad and Fahimeh Khakzad for access and training on contact angle measurements. We appreciate assistance in polymer synthesis, degradation, and characterization from Mohammad Daniyal, Tammy Hendrix-Doucette, Cristian Oviedo, and Yu-Ming Sheu. We thank Hongda Cao for assistance with NMR analysis.

Electronic Supplementary Information

Electronic Supplementary Information (ESI) available: ^{1}H NMR and ^{13}C NMR data obtained from VA (Figure S1); ^{13}C NMR data obtained from EVA and AVA (Figure S2); Curing of EVA, ESA, E4HBA, ESO and DGEBA with MHHPA (catalyzed by 1-MI) to form an epoxy resin (Schemes S1-S5); DSC and TGA data obtained from the EVA monomer (Figure S3); TGA data obtained from epoxy resins containing different ESO and DGEBA contents (Figure S4); T_g as a function of post-curing time for EVA- and ESO-based epoxy resins (Figure S5); Optical

microscopy images of epoxy resins before second-stage curing with differing ESO content (wt% ESO is the ESO content relative to the total amount of ESO and DGEBA) (Figure S6); Fourier transform of optical micrographs for an epoxy resin containing 40 wt% ESO and particle size distributions obtained through image analysis of optical micrographs (Figure S7); SEM images of ESO-based and DGEBA-based epoxy resins (Figure S8); Closer view of mass spectra obtained from degradation products of an ESO-based epoxy resin (Figure S9); Proposed chemical structures and molecular weight for peaks detected in Mass Spectrometry (Table S1); Discussion of solid-state kinetics models. Comparison of different solid-state kinetics models for fitting ESA and 40% ESO-based epoxy resins (Figure S10 and Table S2) Discussion of contracting volume model derivation. FTIR results of EVA and ESO curing reactions (Figure S11). Conversion of epoxy resins quantified through FTIR (Table S3).

References

1. R. Geyer, J. R. Jambeck and K. L. Law, *Science Advances*, 2017, **3**.
2. M. Hong and E. Y. X. Chen, *Green Chemistry*, 2017, **19**, 3692-3706.
3. S. J. Pickering, *Composites Part A: Applied Science and Manufacturing*, 2006, **37**, 1206-1215.
4. R. Bagheri, B. T. Marouf and R. A. Pearson, *Polymer Reviews*, 2009, **49**, 201-225.
5. F. Hussain, M. Hojjati, M. Okamoto and R. E. Gorga, *Journal of Composite Materials*, 2006, **40**, 1511-1575.
6. L. Canesi and E. Fabbri, *Dose-response : a publication of International Hormesis Society*, 2015, **13**, 1559325815598304-1559325815598304.
7. C. Erler and J. Novak, *Journal of Pediatric Nursing*, 2010, **25**, 400-407.
8. J. R. Rochester, *Reproductive Toxicology*, 2013, **42**, 132-155.
9. L. N. Vandenberg, M. V. Maffini, C. Sonnenschein, B. S. Rubin and A. M. Soto, *Endocrine reviews*, 2009, **30**, 75-95.
10. H. Miyagawa, M. Misra, L. T. Drzal and A. K. Mohanty, *Polymer Engineering & Science*, 2005, **45**, 487-495.
11. S.-J. Park, F.-L. Jin and J.-R. Lee, *Macromolecular Chemistry and Physics*, 2004, **205**, 2048-2054.
12. S. G. Tan and W. S. Chow, *Polymer-Plastics Technology and Engineering*, 2010, **49**, 1581-1590.
13. C. S. Ilardo and B. O. Schoepfie, *Industrial & Engineering Chemistry*, 1960, **52**, 323-324.
14. S. Kumar, S. K. Samal, S. Mohanty and S. K. Nayak, *Industrial & Engineering Chemistry Research*, 2017, **56**, 687-698.
15. M. Qi, Y.-J. Xu, W.-H. Rao, X. Luo, L. Chen and Y.-Z. Wang, *RSC Advances*, 2018, **8**, 26948-26958.
16. X. Pan, P. Sengupta and D. C. Webster, *Green Chemistry*, 2011, **13**, 965-975.
17. H. Kishi, A. Fujita, H. Miyazaki, S. Matsuda and A. Murakami, *Journal of Applied Polymer Science*, 2006, **102**, 2285-2292.
18. J. Hong, D. Radojčić, M. Ionescu, Z. S. Petrović and E. Eastwood, *Polymer Chemistry*, 2014, **5**, 5360-5368.
19. J. Łukaszczyk, B. Janicki and M. Kaczmarek, *European Polymer Journal*, 2011, **47**, 1601-1606.
20. A. Devi and D. Srivastava, *European Polymer Journal*, 2007, **43**, 2422-2432.
21. R. Yadav and D. Srivastava, *Journal of Applied Polymer Science*, 2009, **114**, 1670-1681.
22. X. Liu, *Preparation of a bio-based epoxy with comparable properties to those of petroleum-based counterparts*, 2012.
23. X. Liu and J. Zhang, *High‐performance biobased epoxy derived from rosin*, 2010.
24. C. Asada, S. Basnet, M. Otsuka, C. Sasaki and Y. Nakamura, *International Journal of Biological Macromolecules*, 2015, **74**, 413-419.
25. R. J. Li, J. Gutierrez, Y.-L. Chung, C. W. Frank, S. L. Billington and E. S. Sattely, *Green Chemistry*, 2018, **20**, 1459-1466.
26. J. Xin, M. Li, R. Li, M. P. Wolcott and J. Zhang, *ACS Sustainable Chemistry & Engineering*, 2016, **4**, 2754-2761.
27. B. A. Miller-Chou and J. L. Koenig, *Progress in Polymer Science*, 2003, **28**, 1223-1270.
28. B. Narasimhan, *Advanced Drug Delivery Reviews*, 2001, **48**, 195-210.

29. G. Pappa, C. Boukouvalas, C. Giannaris, N. Ntaras, V. Zografos, K. Magoulas, A. Lygeros and D. Tassios, *Resources, Conservation and Recycling*, 2001, **34**, 33-44.
30. C. Busatto, E. Berkenwald, N. Mariano, N. Casis, J. Luna and D. Estenoz, *Polymer Degradation and Stability*, 2016, **125**, 12-20.
31. C. Busatto, J. Pesoa, I. Helbling, J. Luna and D. Estenoz, *Journal of Applied Polymer Science*, 2017, **134**, 45464.
32. F. Iñiguez-Franco, R. Auras, G. Burgess, D. Holmes, X. Fang, M. Rubino and H. Soto-Valdez, *Polymer*, 2016, **99**, 315-323.
33. H. M. Khanlou, P. Woodfield, J. Summerscales, G. Francucci, B. King, S. Talebian, J. Foroughi and W. Hall, *Measurement*, 2018, **116**, 367-372.
34. E. Marten, R.-J. Müller and W.-D. Deckwer, *Polymer Degradation and Stability*, 2003, **80**, 485-501.
35. P. Polyák, E. Urbán, G. N. Nagy, B. G. Vértessy and B. Pukánszky, *Enzyme and Microbial Technology*, 2019, **120**, 110-116.
36. K. Sevim and J. Pan, *Acta Biomaterialia*, 2018, **66**, 192-199.
37. R. Shine, R. Neghabat Shirazi, W. Ronan, C. A. Sweeney, N. Kelly, Y. A. Rochev and P. E. McHugh, *Journal of Medical Devices*, 2017, **11**, 021007-021007-021012.
38. N. A. Weir, F. J. Buchanan, J. F. Orr, D. F. Farrar and G. R. Dickson, *Proceedings of the Institution of Mechanical Engineers, Part H: Journal of Engineering in Medicine*, 2004, **218**, 321-330.
39. H. Antheunis, J.-C. van der Meer, M. de Geus, A. Heise and C. E. Koning, *Biomacromolecules*, 2010, **11**, 1118-1124.
40. R. P. Batycky, J. Hanes, R. Langer and D. A. Edwards, *Journal of Pharmaceutical Sciences*, 1997, **86**, 1464-1477.
41. A. Göpferich, *Biomaterials*, 1996, **17**, 103-114.
42. A. Göpferich, *Macromolecules*, 1997, **30**, 2598-2604.
43. A. Gopferich and R. Langer, *Macromolecules*, 1993, **26**, 4105-4112.
44. J. A. Tamada and R. Langer, *Proceedings of the National Academy of Sciences of the United States of America*, 1993, **90**, 552-556.
45. N. Grassie, M. I. Guy and N. H. Tennent, *Polymer Degradation and Stability*, 1986, **14**, 125-137.
46. N. Tudorachi and F. Mustata, *Arabian Journal of Chemistry*, 2017.
47. R. D. Patel, R. G. Patel and V. S. Patel, *Thermochimica Acta*, 1988, **128**, 149-156.
48. L. Barral, J. Cano, A. J. López, J. Lopez, P. Nógueira and C. Ramírez, *Thermochimica Acta*, 1995, **269-270**, 253-259.
49. P.-Y. Kuo, L. de Assis Barros, Y.-C. Sheen, M. Sain, J. S. Y. Tjong and N. Yan, *Journal of Analytical and Applied Pyrolysis*, 2016, **117**, 199-213.
50. M. Natarajan and S. C. Murugavel, *Polymer Bulletin*, 2017, **74**, 3319-3340.
51. R. L. Shogren, Z. Petrovic, Z. Liu and S. Z. Erhan, *Journal of Polymers and the Environment*, 2004, **12**, 173-178.
52. A. Tarzia, J. Montanaro, M. Casiello, C. Annese, A. Nacci and A. Maffezzoli, *Synthesis, Curing, and Properties of an Epoxy Resin Derived from Gallic Acid*, 2017.
53. J. Xin, P. Zhang, K. Huang and J. Zhang, *RSC Advances*, 2014, **4**, 8525-8532.
54. W. Dang, M. Kubouchi, S. Yamamoto, H. Sembokuya and K. Tsuda, *Polymer*, 2002, **43**, 2953-2958.

55. Y. Sato, Y. Kondo, K. Tsujita and N. Kawai, *Polymer Degradation and Stability*, 2005, **89**, 317-326.
56. G. Oliveux, L. O. Dandy and G. A. Leeke, *Polymer Degradation and Stability*, 2015, **118**, 96-103.
57. T. Liu, M. Zhang, X. Guo, C. Liu, T. Liu, J. Xin and J. Zhang, *Polymer Degradation and Stability*, 2017, **139**, 20-27.
58. T. Liu, X. Guo, W. Liu, C. Hao, L. Wang, W. C. Hiscox, C. Liu, C. Jin, J. Xin and J. Zhang, *Green Chemistry*, 2017, **19**, 4364-4372.
59. G. Jiang, S. J. Pickering, E. H. Lester and N. A. Warrior, *Industrial & Engineering Chemistry Research*, 2010, **49**, 4535-4541.
60. N. Destais-Orvoën, G. Durand and G. Tersac, *Polymer*, 2004, **45**, 5473-5482.
61. K. El Gersifi, N. Destais-Orvoën, G. Durand and G. Tersac, *Polymer*, 2003, **44**, 3795-3801.
62. K. El Gersifi, G. Durand and G. Tersac, *Polymer Degradation and Stability*, 2006, **91**, 690-702.
63. X. Kuang, Q. Shi, Y. Zhou, Z. Zhao, T. Wang and H. J. Qi, *RSC Advances*, 2018, **8**, 1493-1502.
64. X. Kuang, Y. Zhou, Q. Shi, T. Wang and H. J. Qi, *ACS Sustainable Chemistry & Engineering*, 2018, **6**, 9189-9197.
65. X. Gong, H. Kang, Y. Liu and S. Wu, *RSC Advances*, 2015, **5**, 40269-40282.
66. Y. Ma and S. Nutt, *Polymer Degradation and Stability*, 2018, **153**, 307-317.
67. I. Okajima, M. Hiramatsu, Y. Shimamura, T. Awaya and T. Sako, *The Journal of Supercritical Fluids*, 2014, **91**, 68-76.
68. S. You, S. Ma, J. Dai, Z. Jia, X. Liu and J. Zhu, *ACS Sustainable Chemistry & Engineering*, 2017, **5**, 4683-4689.
69. N. Grassie, M. I. Guy and N. H. Tennent, *Polymer Degradation and Stability*, 1986, **14**, 209-216.
70. A. Dupuis, F.-X. Perrin, A. Ulloa Torres, J.-P. Habas, L. Belec and J.-F. Chailan, *Polymer Degradation and Stability*, 2017, **135**, 73-84.
71. L. Zhao, L. Zhang and Z. Wang, *RSC Advances*, 2015, **5**, 95126-95132.
72. C. Yu, Z. Xu, Y. Wang, S. Chen, M. Miao and D. Zhang, *ACS Omega*, 2018, **3**, 8141-8148.
73. T. Liu, C. Hao, L. Wang, Y. Li, W. Liu, J. Xin and J. Zhang, *Macromolecules*, 2017, **50**, 8588-8597.
74. S. Wang, S. Ma, Q. Li, X. Xu, B. Wang, W. Yuan, S. Zhou, S. You and J. Zhu, *Green Chemistry*, 2019, **21**, 1484-1497.
75. S. Ma, J. Wei, Z. Jia, T. Yu, W. Yuan, Q. Li, S. Wang, S. You, R. Liu and J. Zhu, *Journal of Materials Chemistry A*, 2019, **7**, 1233-1243.
76. G. Yang, B. J. Rohde and M. L. Robertson, *Green Materials*, 2013, **1**, 125-134.
77. M. Janvier, L. Hollande, A. S. Jaufurally, M. Pernes, R. Ménard, M. Grimaldi, J. Beaugrand, P. Balaguer, P.-H. Ducrot and F. Allais, *ChemSusChem*, 2017, **10**, 738-746.
78. Q. Zhang, M. Molenda and T. M. Reineke, *Macromolecules*, 2016, **49**, 8397-8406.
79. Q. Zhang, H. R. Phillips, A. Purchel, J. K. Hexum and T. M. Reineke, *ACS Sustainable Chemistry & Engineering*, 2018, **6**, 14967-14978.
80. S. Ma and D. C. Webster, *Macromolecules*, 2015, **48**, 7127-7137.
81. A. Ruiz de Luzuriaga, R. Martin, N. Markaide, A. Rekondo, G. Cabañero, J. Rodríguez and I. Odriozola, *Materials Horizons*, 2016, **3**, 241-247.

82. G. Yang, B. J. Rohde, H. Tesefay and M. L. Robertson, *ACS Sustainable Chemistry & Engineering*, 2016, **4**, 6524-6533.
83. S. S. Umare and A. S. Chandure, *Chemical Engineering Journal*, 2008, **142**, 65-77.
84. M. Fache, R. Auvergne, B. Boutevin and S. Caillol, *European Polymer Journal*, 2015, **67**, 527-538.
85. S. H. Ghaffar and M. Fan, *International Journal of Adhesion and Adhesives*, 2014, **48**, 92-101.
86. C. Aouf, H. Nouailhas, M. Fache, S. Caillol, B. Boutevin and H. Fulcrand, *European Polymer Journal*, 2013, **49**, 1185-1195.
87. J. D. Espinoza-Perez, B. A. Nerenz, D. M. Haagenson, Z. Chen, C. A. Ulven and D. P. Wiesenborn, *Polymer Composites*, 2011, **32**, 1806-1816.
88. F. Mustata, N. Tudorachi and D. Rosu, *Composites Part B: Engineering*, 2011, **42**, 1803-1812.
89. F. v. Burkersroda, L. Schedl and A. Göpferich, *Biomaterials*, 2002, **23**, 4221-4231.
90. H. Antheunis, J.-C. van der Meer, M. de Geus, W. Kingma and C. E. Koning, *Macromolecules*, 2009, **42**, 2462-2471.
91. T. Walter, J. Augusta, R.-J. Müller, H. Widdecke and J. Klein, *Enzyme and Microbial Technology*, 1995, **17**, 218-224.
92. X. Zhu and R. D. Braatz, *Journal of biomedical materials research. Part A*, 2015, **103**, 2269-2279.
93. A. Khawam and D. R. Flanagan, *The Journal of Physical Chemistry B*, 2006, **110**, 17315-17328.
94. Y. Xia and R. C. Larock, *Green Chemistry*, 2010, **12**, 1893-1909.
95. Q. Liu, L. Jiang, R. Shi and L. Zhang, *Progress in Polymer Science*, 2012, **37**, 715-765.
96. E. Crawford and A. J. Lesser, *Journal of Polymer Science Part B: Polymer Physics*, 1998, **36**, 1371-1382.

TOC Graphic

Biobased epoxy resins, derived from lignin, phenolic acids, and vegetable oils, exhibited rapid degradation through hydrolysis in basic solution.